Results in Engineering 25 (2025) 104380

Contents lists available at ScienceDirect

Results in Engineering

journal homepage: www.sciencedirect.com/journal/results-in-engineering

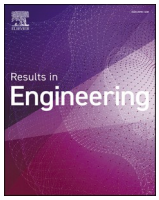

Research paper

Evaluation of the effects of corrosion of carbon steel in acid mine drainages by using an explainable artificial intelligence model.

María Luisa de la Torre [a,b,*], Javier Aroba [c,d], Jose Miguel Davila [a,e], Aguasanta M. Sarmiento [a,e]

[a] Department of Mining, Mechanical, Energy and Construction Engineering, University of Huelva 21071 Huelva, Spain
[b] Natural Resources, Health and Environment Research Centre (RENSMA), University of Huelva, Spain
[c] Department of Information Technologies, University of Huelva 21007, Huelva, Spain
[d] Center for Advanced Studies in Physics, Mathematics and Computing (CEAFMC), University of Huelva 21007, Huelva, Spain
[e] Science and Technology Centre of Huelva (CCTH), University of Huelva, Spain

ARTICLE INFO

Keywords:
Acid mine drainage
Artificial intelligence
Carbon steel
Corrosion
Fuzzy logic
Mining facilities

ABSTRACT

One of the main problems faced by sulfide mining facilities is the corrosion of steel caused by acidic leachates, a process that is further accelerated by the presence of acidophilic bacteria that act as catalysts in the reaction. This study presents an AI-based approach to assess acid mine drainage as a result of corrosion, adding novelty to the study by using it alongside Fuzzy Logic, obtaining qualitative models based on fuzzy rules that corroborate and expand on the contributions of statistical techniques. In a laboratory experiment, S-235JR (EN 10025) carbon steel samples were immersed for 26 days in four solutions: two with a high Fe^{2+}/Fe^{3+} ratio, one from a mine with acidophilic bacteria (with an initial Fe^{2+} concentration of 1390 mg/L) and one synthetic without bacteria (Fe^{2+} concentration of 1961 mg/L); one from a mine with a high Fe^{3+}/Fe^{2+} ratio (with an initial Fe^{2+} concentration of 0.10 mg/L) and distilled water simulating rain effects. Results showed a greater increase in Fe concentration in solutions with a higher initial Fe^{2+}/Fe^{3+} ratio (with an increase rate higher than 2). All acidic solutions eventually became anoxic, with a slower transition in the bacteria-free solution. Cu concentration dropped sharply in all cases, regardless of bacteria presence or Fe ratios, likely because the net acidity kept Cu in solution for a longer time. In the synthetic solution without bacteria, pH gradually increased as steel oxidation proceeded more slowly. In contrast, solutions with bacteria showed a sharp pH rise in the early hours of the experiment.

1. Introduction

1.1. Acid mine drainage and steel corrosion

Polymetallic sulfide mining, and more specifically iron sulfide mining, generates an acidic leachate (Acid Mine Drainage, AMD) with a high concentration of sulfates and dissolved metals, which represents a global problem [1,2]. This issue arises not only from the pollution it causes, directly affecting water bodies, but also from the numerous indirect problems it generates. Corrosion of metals is an electrochemical process in which the metal is converted into an oxide or any other compound with a higher oxidation number [3]. One of the indirect problems of AMD is the acceleration of the steel corrosion process [4]. Steel is one of the most widely used materials in this industry across all its exploitation stages (extraction, mineral processing, and metallurgy). Steel and aluminium degradation is a serious problem for mining companies that profit from polymetallic sulphides at all stages of mining. Mobile machinery, support structures of mineral processing facilities, crushing, grinding, regrinding, classifying machinery, etc., are also subjected to these environments. Other auxiliary machinery such as pumping and ventilation equipment, augers and drilling/blasting equipment, control panels, etc., can also be affected [4]. According to a US survey, corrosion costs six cents for every dollar of gross domestic product in the United States. Globally, this amounts to over US$4 trillion annually [5], making it essential to understand corrosion processes in order to provide valuable anti-corrosion recommendations.

The process of Acid Mine Drainage generation occurs when metallic sulfides, initially in anaerobic conditions, are exposed to atmospheric oxygen and water. This exposure triggers a series of reactions that generate sulfates, iron precipitates, and hydrogen ions, leading to a

* Corresponding author.
E-mail address: mltorre@uhu.es (M.L. de la Torre).

https://doi.org/10.1016/j.rineng.2025.104380
Received 15 January 2025; Received in revised form 13 February 2025; Accepted 15 February 2025
Available online 23 February 2025

decrease in the pH of the water. This global reaction involves several intermediate steps, including the oxidation of Fe^{2+} to Fe^{3+}, hydrolysis of Fe^{3+} which generates more acidity and iron precipitates, and under these acidic conditions, the oxidation of pyrite by Fe^{3+} itself, producing more acidity, sulfates, and Fe^{2+}.

The oxidation rate of Fe^{2+} is very slow; however, in natural environments, it can be increased by 10^4 to 10^6 times by Iron-oxidizing bacteria (FeOBs) [6–9], such as Thiobacillus ferrooxidans, Leptospirillum ferrooxidans, etc., which act as catalysts for the oxidation of ferrous ions [10]. These microorganisms are among the primary contributors to metal corrosion (Microbiologically Influenced Corrosion, MIC), being involved in the electrochemical processes of corrosion [11, 12]. For this reason, acid mine drainage is highly oxidative, with redox potentials that can exceed 700 mV [13].

Furthermore, many other sulfides have oxidation products that release elements such as arsenic, copper, cobalt, cadmium, chromium, mercury, nickel, lead, etc. In addition, the acid hydrolysis of the host rocks through which these acidic leachates flow introduces elements into the solution, in varying abundances, such as Ca, Al, Mg, Mn, K, Na, etc. Consequently, such acidic leachates can contain concentrations of up to 60,000 mg/L of Fe, 2400 mg/L of Al, 860 mg/L of Zn, 800 mg/L of Cu, 742 mg/L of As, 187,000 mg/L of sulfates, among others, and pH values that can even reach negative values [14], serving as an elemental indicator of the medium's aggressiveness.

1.2. Explainable AI model based on fuzzy logic

Currently, Explainable Artificial Intelligence [15] provides techniques such as fuzzy logic (FL), which, in situations with a certain degree of uncertainty, outperforms results obtained through classical statistical methods [16,17]. While classical statistical models or numerical simulations can be effective in identifying patterns or predicting behaviors, fuzzy logic allows for a more natural and understandable representation of the uncertainty and imprecision inherent in complex systems like corrosion. By combining AI-based methods and fuzzy logic, it is possible to build qualitative rule-based models that are easily interpretable by experts, facilitating the understanding of underlying processes and enabling more informed decisions. This overcomes the limitations of traditional approaches, which often lack the flexibility and transparency needed to adapt to the variability and complexity of corrosion systems. AI-driven algorithms have proven to stand out for their ability to handle large datasets more precisely and quickly in various fields ([18–20])

Specifically, fuzzy logic (FL) mathematically describes how humans engage with the environment and make choices. Consequently, models utilizing fuzzy logic can handle uncertain data using fuzzy sets, enabling the modeling of complex non-linear processes and deriving insights from data through various machine learning algorithms [21]. In this manner, FL models serve as an excellent option for data processing in environmental science contexts [22–25]. Traditional corrosion prediction methods, though beneficial, frequently fall short in effectively accounting for the intricate interactions among chemical, physical, and environmental factors that determine corrosion rates [26]. In the last decade, machine learning (ML) has been employed in a number of corrosion-related problems, such as for modeling CO2 corrosion, detecting corrosion from automated image analysis, modeling corrosion defect growth in pipelines, material inspection, modeling corrosion rate in marine environment or finding corrosion initiation time of embedded steel in reinforced concrete [26–33] but no references have been found where AI model based on fuzzy logic is applied to the study of corrosion caused by acid mine drainage.

1.3. Objective

This research paper introduces an innovative Artificial Intelligence (AI)-based approach to evaluate the effects of carbon steel corrosion in acid mine drainage. The proposed methodology [34] introduces novelty by using AI techniques along with Fuzzy Logic, obtaining qualitative models based on fuzzy rules that are very easy to interpret and which corroborate and expand upon what is provided by statistical techniques.

2. Materials and methods

2.1. Laboratory experiment

A laboratory experiment was conducted in which four plastic containers were prepared, each containing a S-235JR (EN 10,025) carbon steel specimens (density: 7.85 g/cm^3), immersed in different solutions for 26 days. The chemical composition (wt%) of the S-235JR carbon steel specimens was as follows: 0.067 % C, 0.53 % Mn, 0.008 % Si, 0.016 % P, 0.013 % S, 0.031 % Al, and Fe as the balance (S/EN 10,204). The coupons were rinsed with distilled water, degreased in absolute ethanol, dried with warm air, and weighed using a precision balance (Radwag, Polska, ±0.01 g). To simulate environmental conditions, the laboratory was maintained at a low temperatura (25 °C), and a light-dark (12:12) cycle was applied. All the specimens were placed vertically within their containers, ensuring that the entire surface remained immersed in the solution at all times.

Each of the plastic containers was filled with a four different solutions because the leachates found in the Iberian Pyrite Belt have different characteristics depending on the geology of the sulfide mass, whether it has been extracted from an underground or open-pit mine, etc.: one with an acidic leachate from the Poderosa mine, with a high Fe^{2+}/Fe^{3+} ratio (hereafter referred to as PO); another with an acidic leachate from the Peña del Hierro mine, with a high Fe^{3+}/Fe^{2+} ratio (hereafter referred to as PH); a third with a synthetic solution replicating AMD with a high Fe^{2+}/Fe^{3+} content but without bacteria (hereafter referred to as ST) in order to discern the differences in behavior when an acidic solution does not contain bacteria that could modify the results; and finally, one with distilled water simulating rainwater (hereafter referred to as BK).

To ensure that the synthetic solution (ST) exhibited physicochemical characteristics comparable to actual acid mine drainage (AMD) samples, arsenic (As), cobalt (Co), chromium (Cr), and nickel (Ni) were introduced using standard solutions for atomic absorption spectroscopy. The pH was adjusted by adding 96% sulfuric acid and relevant salts. The corresponding salts—$FeSO_4{\cdot}7H_2O$, $CuSO_4{\cdot}5H_2O$, $Pb(NO_3)_2$, $ZnSO_4{\cdot}7H_2O$, $Al_2(SO_4)_3$, $CaCl_2$, $MgSO_4{\cdot}7H_2O$, K_2SO_4, NaCl, and $MnSO_4$—were accurately weighed and dissolved in deionized water, following the methodology described by Orandi and Lewis [35]. Trace elements (As, Co, Cr, and Ni) were incorporated using standard atomic absorption solutions, and the final pH was adjusted with 96 % sulfuric acid to achieve the desired conditions.

Every 24 hours, the physicochemical parameters of each solution were measured (temperature, pH, specific conductance, redox potential, and dissolved oxygen). Temperature, pH, and specific conductance were measured using a multiparametric portable device (Crison MM40). Dissolved O_2 was analyzed with a Hanna meter, and the redox potential was determined using a Hanna meter with Pt and Ag/AgCl electrodes (Crison). The pH meter was calibrated using Hanna standard solutions (pH 4.01 and pH 7.01), and the redox potential was checked using Hanna standard solutions (240 mV and 470 mV).

Also, every 24 h, a 10 mL sample of each solution was taken for analysis of dissolved elements. The water samples were filtered, at the time of collection, through 0.22 μm Millipore filters mounted on Sartorius polycarbonate filter holders, acidified to pH < 2 with suprapur HNO_3 (2 %), and stored in the dark at 4°C in polyethylene bottles until analysis. Samples for Fe^{2+} determination were filtered through 0.22 μm, and Fe^{2+} was complexed by adding a 0.5 % (w/w) 1,10-phenanthroline chloride solution after buffering to pH 4.5 with an ammonium acetate/acetic acid buffer [36].

For each sample collected daily, the concentration of elements was analyzed using an Agilent Technologies 7700 Series inductively coupled

plasma mass spectrometer (ICP-MS) and an Iris Intrepid Model atomic emission spectrometer (ICP-AES). Detection limits were calculated using the average and standard deviations from ten blanks and were as follows: 100 μg/L for Al, Ca, Fe, Mn, Mg, Na, K, Si; 50 μg/L for Zn; 5 μg/L for Cu; 2 μg/L for As; and 1 μg/L for other trace elements. Iron species were determined using colorimetry at 510 nm with a SHIMADZU UVmini-1240 spectrophotometer. The detection limit was 0.3 mg/L, with precision better than 5 %. Speciation analysis of the samples was carried out with the assistance of the equilibrium chemical-speciation/mass transfer model PHREEQC [37] using the thermodynamic database WATEQ4F [38].

Finally, for each sample, the net acidity was calculated [39], as defined by the widely cited equation for calculating Acidity in units of mg/L as $CaCO_3$, where metal concentrations are in mg/L:

$$\text{Acidity}_{\text{calculated}} = 50\left(\left(2Fe^{2+}/56\right) + \left(3Fe^{3+}/56\right) + 3(Al/27) + (2Mn/55) + 1000\ \left(10^{-pH}\right)\right)$$

2.2. Explained artificial intelligence: fuzzy logic approach

AI has reached significant levels of applicability in recent years. Among AI techniques, those that we can understand (as opposed to those dominated by subsymbolic methods, such as ensembles or deep neural networks) are particularly relevant in many areas. Understanding how an AI technique works allows us to interpret the knowledge algorithms have acquired through machine learning models and apply it in our own context. This field, currently known as eXplainable Artificial Intelligence (XAI) [40,41], includes techniques like fuzzy logic, which has traditionally been successful in solving practical problems by using linguistic terms to express its definitions [15].

Among eXplainable Artificial Intelligence (XAI) techniques, fuzzy logic stands out [19]. It has achieved success in solving practical problems by expressing real-world concepts and definitions using linguistic terms. Specifically, fuzzy rules models, which rely on fuzzy logic, are common and well-known. In this study, we'll utilize a fuzzy rules model obtained through clustering algorithms, as detailed in the upcoming subsection.

2.2.1. Fuzzy clustering

The primary goal of clustering algorithms, as outlined by Kaufmann and others [42], is to organize a collection of data into clusters or groups. Within these clusters, the data points are more closely related to each other based on a specific metric than to those in other clusters. Traditional clustering techniques assign each data point to a single cluster, resulting in a binary membership status: either 0 (not a member) or 1 (a member). On the other hand, fuzzy clustering methods [43], allow data points to belong to multiple clusters simultaneously. Here, the degree of membership for a data point in any given cluster is expressed as a number between 0 and 1, indicating a gradient of belonging. This approach enhances the granularity of classification and improves the flexibility in grouping data points.

2.2.2. Proposed fuzzy logic approach

The proposed approach using fuzzy logic [34] relies on the methodology outlined in [44]. It aims to construct fuzzy models based on the fuzzy C-Means algorithm [45,46], resulting in IF-THEN fuzzy rules of the form: IF x ∈ A THEN y ∈ B. Here, x =(x1, x2,….xn) represents input variables (antecedents), A=(A1,A2, ….An) represents n fuzzy sets, y is the output variable (consequent), and B is a fuzzy set for this output variable.

Before processing the data, the initial step involves identifying the variables within the dataset that require study. These selected variables will serve as the consequents in the fuzzy rules to be generated. The remaining parameters in the dataset will function as antecedents in these rules. Subsequently, the proposed methodology automatically analyzes the dataset, clustering the consequent parameters into an optimal number of fuzzy clusters [47]. Once the consequent parameters are clustered, each fuzzy cluster is projected onto the antecedent space [44], determining the membership grade of the antecedents for each cluster. Finally, based on the information obtained from these steps, a set of graphical IF-THEN fuzzy rules is generated, as illustrated in Fig. 1, where the antecedent variables are A1 and A2, and the consequent variable is C.

The fuzzy rule associated with Fig. 1 can be understood in natural language as follows:

IF A1 is small or big AND A2 is average, THEN C is very small.

However, this fuzzy rule also can be interpreted as:

C is very small, IF A2 is small or big AND A2 is average

The proposed fuzzy approach has been created to be used on multiple-parameter numeric datasets, producing a fuzzy rule-based system without manual intervention. This system provides a descriptive model of the analyzed data.

3. Results and discussion

Table 1. Initial chemical composition of the AMD-solutions (EC: specific conductance. NA: net acidity). Values in μg/L except Al, Ca, Cu, Fe, Fe2+, K, Mg, Na, S, Si and Zn in mg/L, EC in mS/cm and NA in mg/L as CaCO3.

The low pH values observed in the three acidic solutions (PH, PO, ST) are notable, along with the high concentrations of sulfur (present as sulfates in the solutions) and iron, as well as the elevated net acidity values, particularly in PH. It is worth highlighting that the Fe^{2+} concentration is significantly higher in PO and ST compared to PH.

To evaluate the behavior of all solutions, a statistical summary was generated, and artificial intelligence (AI) techniques were applied exclusively to the measurements of physicochemical parameters and dissolved elements that exhibited temporal variation across all solutions.

3.1. Statistical summary

Table 2. Statistical summary of the measured parameters and dissolved elements analyzed in each solution (Values in μg/L except Al, Ca, Cu, Fe, Fe^{2+}, K, Mg, Na, S, Si, and Zn in mg/L, EC in mS/cm, and NA in mg/L as $CaCO_3$). EC: electrical conductance, Eh: redox potential, DO: dissolved oxygen.

In the case of distilled water, which aims to replicate the effect of rainwater in the laboratory, the pH ranges from a minimum value of 5 to a maximum value of 5.9, indicating that it is a moderately acidic solution. It exhibits very low conductivity. Regarding the dissolved elements analyzed, it can be observed that the minimum values in many cases fall below the detection limits, except for K, S, Ni, Sr, and Zn. Meanwhile, the maximum values show an increase, with all cases exceeding the detection limits, especially Fe^{2+}, which reaches a maximum of 15.8 mg/L, and Mn, at 26.1 μg/L. This suggests oxidation of the steel plate, although to a lesser extent than in the more acidic solutions. It is also

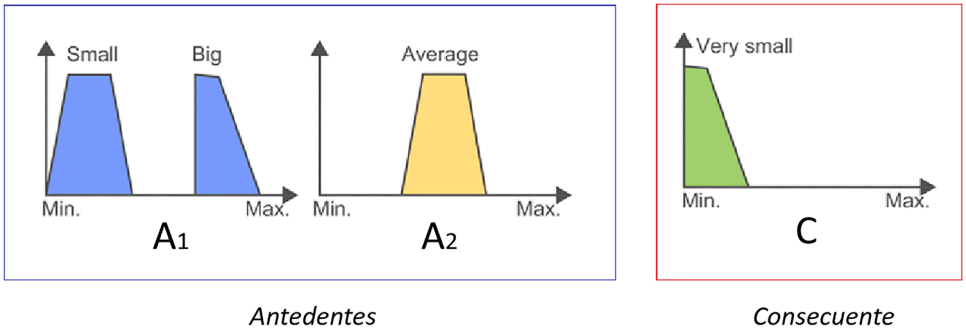

Fig. 1. Example of graphical IF–THEN fuzzy rule.

Table 1
presents the initial results of the measurements of physicochemical parameters and the analysis of dissolved elements in each of the solutions.

	BK	PH	PO	ST		BK	PH	PO	ST
pH	5	1.44	1.78	1.51	Ga	<0.5	1327	217	<15
EC	0.03	29.5	13.51	30.0	Gd	<0.5	738	510	<15
Al	<0.1	3766	431	1323	Ge	<0.5	482	109	<15
Ca	<0.1	19.1	123	145	La	<0.5	2232	1000	<15
Cu	<0.1	15.6	118	69.6	Li	<0.5	5464	222	<15
Fe	<0.1	22,147	1930	2278	Mo	<0.5	767	45.2	<15
Fe^{2+}	0.10	330	1390	1961	Nd	<0.5	3036	1603	<15
K	0.5	<2	18.3	3.5	Ni	<0.5	1242	142	305
Mg	<0.1	2118	165	210	Pb	<0.5	25.3	275	3041
Mn	<0.5	27.3	5.53	1.57	Pr	<0.5	713	363	<15
Na	<0.1	0.1	19.7	11.0	*Sc*	<0.5	219	78.0	<15
S	0.3	26,292	2816	5180	Se	<0.5	786	393	<15
Si	<0.1	65.1	40.3	<0.1	Sm	<0.5	730	428	<15
Zn	3.60	14.6	83.4	127	Sr	<0.5	234	164	<15
As	<0.5	12,547	3789	1257	Th	<0.5	404	102	<15
Cd	<0.5	114	376	<0.5	Ti	<0.5	230	106	<15
Ce	<0.5	5476	2714	<0.5	V	<0.5	132	65.9	<15
Co	<0.5	20,429	1438	75.9	Y	<0.5	1317	1530	<15
NA	1.24	52,413	6814	13,175					

noteworthy that the variance is generally low due to the limited variability in the analyzed concentrations, with significant variation only observed in the cases of Eh, Fe^{2+}, and Mn.

With respect to of the acidic solutions, the one with the highest initial Fe concentration, one of the main products of metal dissolution in these acidic environments, is PH, ranging from a minimum of 22,147.5 mg/L to 41,246.9 mg/L, representing an increase of 1.8 times the initial concentration. In the case of PO, the concentration of this element starts at a minimum of 1930.11 mg/L and reaches 4503.65 mg/L (a ratio of 2.3). In the ST solution, it increases from 2278.47 mg/L to 6363.54 mg/L (a ratio of 2.79). When comparing the different solutions, it is observed that the relative increase in Fe concentration is higher in PO and ST than in PH due to a higher initial concentration of Fe^{3+} and total acidity in the latter. This leads to a greater increase in hydroxylated species in solution, which subsequently precipitate onto the steel surface as oxyhydroxysulfates. Fe^{3+} formed schwertmannite (pH 2.5–3.5) or jarosite (pH 1.8–3.0) in the presence of FeOBs. The formation of schwertmannite or jarosite is an acid-producing process that competes with the hydrolysis of Fe^{2+} [9].

The concentration of Fe^{2+} and Fe^{3+} is closely linked to corrosion rates, as Fe^{2+} is formed when the metal dissolves in acidic environments, while Fe^{3+} is the product of the oxidation of Fe^{2+}, accelerating the corrosion process. The presence of bacteria, such as Acidithiobacillus ferrooxidans, speeds up the conversion of Fe^{2+} to Fe^{3+}, which increases corrosion by generating a feedback cycle where Fe^{3+} acts as a strong oxidizing agent. In this context, an increase in the concentration of Fe^{3+}, facilitated by bacterial activity, generally results in a higher corrosion rate. If we focus on what happens with Fe^{2+}, which is a product of metal dissolution in acidic environments and plays a key role in electrochemical corrosion reactions in each solution, we can observe that for PH, the minimum concentration is 330 μg/L, reaching a maximum of 7425 μg/L (a ratio of 22.5). PO starts with a higher Fe^{2+} concentration of 1390 μg/L, reaching 3970 μg/L (a ratio of 2.8), and ST ranges from 1961.2 μg/L to 6000 μg/L (a ratio of 3). In other words, in the solution with the highest Fe^{3+}/Fe^{2+} content (PH), the increase in Fe^{2+} is much more significant than in PO or ST. This is a consequence of steel oxidation and the activity of acidophilic bacteria. The Fe^{2+} will be transformed to Fe^{3+} by the FeOBs, and the consumption of Fe^{2+} will accelerate the conversion of Fe^{0} to Fe^{2+}, thereby accelerating corrosion [8]. The variance of Fe and Fe^{2+} is very high both in PH and ST (reaching values of 107), unlike in PO, where the value is around 28,000.

It is interesting to note that the minimum DO value in the case of the acidic solutions is 0, reaching a maximum of 56.6% in PH and 56.5 % in PO, while in ST, the maximum is 77.3 %. Oxygen is consumed in the iron oxidation reactions, but additionally, oxygen, as an electron acceptor, provides energy to the FeOBs for their metabolic processes [8]. Therefore, the oxygen depletion rate is lower in the solution that does not contain bacteria. These bacteria consume oxygen, and once it reaches anoxic conditions, they begin to consume Fe, which increases oxygen levels again until it decreases and the process repeats. The metabolic versatility of microorganisms associated with iron mounds (and AMD, in general) allows them to engage in Fe^{2+} oxidation or Fe^{3+} reduction depending on the availability of O_2 (or its absence) [6]. Fe^{3+}-reducing bacteria can reduce Fe^{3+} to Fe^{2+} under anoxic conditions using electron donors such as hydrogen (H_2) [48].

Another element that shows a significant difference between maximum and minimum values is Cu. In the case of PH, the minimum concentration is 370.965 mg/L and the maximum is 15,643.6 mg/L (a ratio of 42.17, representing a decrease, as observed in the following section with the application of AI). In PO, the minimum is 645.04 mg/L

Table 2
presents the statistical summary of the monitored parameters in each solution, highlighting significant differences between them.

	Parameter	Median	Variance	Mínimum	Maximum
DISTILLED WATER (BK)	pH	5.48	0.0415719	5	5.9
	EC	0.045	0.00086407	0.014	0.12
	Eh	292	4226.82	145	354
	DO	50.2	279.969	21.8	92.1
	T	17.1	1.50605	14.5	19.3
	Ca	0.33	0.0155632	<0.1	0.57
	Fe	1.63	0.575212	<0.1	2.9
	Fe^{2+}	13.94	33.5923	<0.1	15.83
	K	3.03	0.988536	0.48	4.92
	S	1.15	0.514317	0.3	7.35
	Cu	0.5	0.566319	<0.1	3.79777
	Li	0.5	0.0543464	<0.5	1.34419
	Mn	15.30	45.1761	<0.5	26.1072
	Ni	1.95	0.161016	0.5	2.55049
	Sr	1.04	0.133631	0.5	1.65561
	Zn	1.69	2.40922	1.16	7.2428
PEÑA DEL HIERRO MINE (PH)	pH	2.55	0.169779	1.44	3.08
	EC	40.5	19.8539	29.5	46.64
	Eh	385	2216	320	545
	DO	2.2	258.552	0	56.6
	T	17.4	1.1113	14.6	18.7
	Ca	21.391	3.48421	19.1247	25.3104
	Fe	32,023.4	2.24E+07	22,147.5	41,246.9
	Fe^{2+}	7350	2.14E+06	330	7425
	K	2.01712	0.288422	1.71304	3.85081
	S	29,413.9	7.56E+06	26,292.8	36,099.5
	Cu	2644.38	1.88E+07	370.965	15,643.6
	Li	7107.2	739,253	5242.9	9441.78
	Mn	53,902.8	1.62E+08	27,262.2	76,991.8
	Ni	1001.88	237,713	282.559	1801.17
	Sr	254.376	712.839	233.701	349.17
	Zn	16,487.4	4.21E+06	14,564.1	22,792.2
PODEROSA MINE (PO)	pH	3.26	0.186802	1.78	3.5
	EC	9.105	1.20508	8.2	13.51
	Eh	360	550.028	330	424
	DO	8.6	272.904	0	56.5
	T	17.4	1.14621	14.7	18.7
	Ca	133.15	122.673	122.06	163.59
	Fe	3536.47	288,196	1930.11	4503.65
	Fe^{2+}	3090	287,211	1390	3970
	K	19.7	2.28868	18.27	24.15
	S	3137.43	54,292.7	2816.74	3754.7
	Cu	2709.44	6.99E+08	645.045	117,972
	Li	293.487	1040.29	221.584	346.275
	Mn	9285.27	5.74E+06	5525.09	15,560.8
	Ni	364.374	3766.82	142.332	441.341
	Sr	188.473	344.581	163.624	236.936
	Zn	94,181.3	7.37E+07	83,381.5	116,457
SYNTETIC SOLUTION (ST)	pH	1.96	0.3744	1.32	3.31
	EC	18.06	20.5406	14.45	30
	Eh	350	603.278	300	388
	DO	38.4	546.762	0	77.3
	T	17.4	1.0226	14.8	18.5
	Ca	148.878	93.2135	137.372	173.065
	Fe	4768.93	1.30E+06	2278.47	6363.54
	Fe^{2+}	4200	1.06E+06	1961.2	6000
	K	3.62448	0.6772	2	5.61165
	S	5621.35	193,236	5180.76	6745.61
	Cu	2646.06	3.09E+08	509.305	69,556
	Li	47.7687	101.234	37.8305	77.8777
	Mn	7793.86	8.95E+06	1573.25	12,596.7
	Ni	641.133	21,416.8	240.848	740.514
	Sr	52.0423	29.9151	44.2933	64.7534
	Zn	130,140	7.35E+07	119,611	150,479

and the maximum is 117,972 mg/L (a ratio of 182.9), while in ST, the minimum is 509.305 mg/L and the maximum is 69,556 mg/L (a ratio of 136.5). That is, it is in the PO solution where the greatest variation in Cu concentration occurs, followed by ST, while the variation in PH is much lower. Cu decreases due to an electrolytic process that leads to its precipitation [49]. This occurs in all cases. In environments with high Fe^{3+} concentration, this ion acts as a strong oxidant that favors the dissolution of steel, promoting the release of Cu. However, the released Cu may subsequently precipitate as copper oxides or hydroxides, or even be adsorbed by suspended iron particles, which would explain a decrease in its concentration in solution. In PH, the precipitation of Cu has a lower ratio due to the high net acidity, which keeps it in solution for a longer time. In all three acidic solutions, the variance of this element is very high.

The PH solution exhibits the highest concentration of sulfur (in the form of sulfates), ranging from a minimum of 26,292.8 mg/L to 36,099.5 mg/L (a ratio of 1.37). In PO, the concentration ranges from 2816.74 mg/L to 3754.7 mg/L (a ratio of 1.3), and in ST, it ranges from 5180.76 mg/L to 6745.61 mg/L (a ratio of 1.3). Therefore, the variation ratio in sulfur concentration is similar across all three solutions. This could be due to the absence of sulfate-reducing bacteria (SRB) that reduce SO_4^{2-} to HS^- [8].

3.2. AI Methodology

Figs. 2, 3, 4, and 5 illustrate the evolution of various parameters analyzed in the samples obtained from each solution (antecedents) in relation to the time that the solution was in contact with the steel (consequent), where oxidation reactions occurred on the steel, which in turn modified the physicochemical properties of the solutions in contact with it. The universe of discourse of each variable, i.e., the values that the variables can take, has at its extreme values the maximum and minimum values obtained analytically.

For this study, data from the 26 total days of the 4 experiments were analyzed and processed, resulting in the four fuzzy rule systems (FRS) shown in Figs. 2, 3, 4, and 5. In the first rule (row 1), the values that each antecedent parameter (pH, EC, Eh, ..., Zn) can take are represented for the first 160 h of study, i.e., 7 days; in the second rule (row 2), for the time interval (160, 325), i.e., 13 days; in the third rule (row 3), for the time interval (325, 485), i.e., 20 days; and finally, in the fourth rule (row 4), for the approximate time interval (485, 624), i.e., 26 days.

Regarding pH, it is observed that, in both PO and PH, the values undergo a sharp change from the initial hours, rising to high to very high values, reaching their maximum at the end of the experiment. However, in ST, the increase is more gradual, with high or very high values reached only after the third part of the experiment. This is because in this latter solution, there are no bacteria, and thus the oxidation reactions of the steel, from Fe^{2+} to Fe^{3+} (with proton consumption and a consequent pH increase), occur more slowly.

In all cases, an increase in Fe is observed, though with different time-dependent behaviors due to the mass loss of the steel specimens [3] caused by corrosion. The increase is more significant in the acidic solutions than in distilled water, although corrosion also occurs in the latter. The Fe^{2+} behavior is similar in PO and ST, progressively increasing throughout the experiment, as these solutions have a higher Fe^{2+}/Fe^{3+} ratio. However, in PH, it can be seen that Fe^{2+} takes almost any value in the first part of the experiment. After that, it rises to higher Fe^{2+} values until the end of the experiment, due to the initial presence of a higher Fe^{3+}/Fe^{2+} ratio, as Fe^{3+} is the strongest oxidant of pyrite in acidic conditions [50], which also increases the Fe^{2+} concentration.

In all cases, it is observed that Cu can take almost any value in the early hours of the experiment. However, after 160 hours, a sharp decrease occurs to very low or low values in all solutions. The drop in copper concentration, due to its possible adsorption or coprecipitation with Fe precipitates, as explained earlier, is rapid and does not depend on the presence of bacteria or the Fe^{2+}/Fe^{3+} ratio.

4. Conclusions

By comparing the evolution of the composition of different acidic solutions, due to the corrosion of steel and its consequent mass loss, a greater relative increase in Fe concentration is observed in solutions with a higher initial Fe^{2+}/Fe^{3+} ratio (PO and ST) compared to the solution

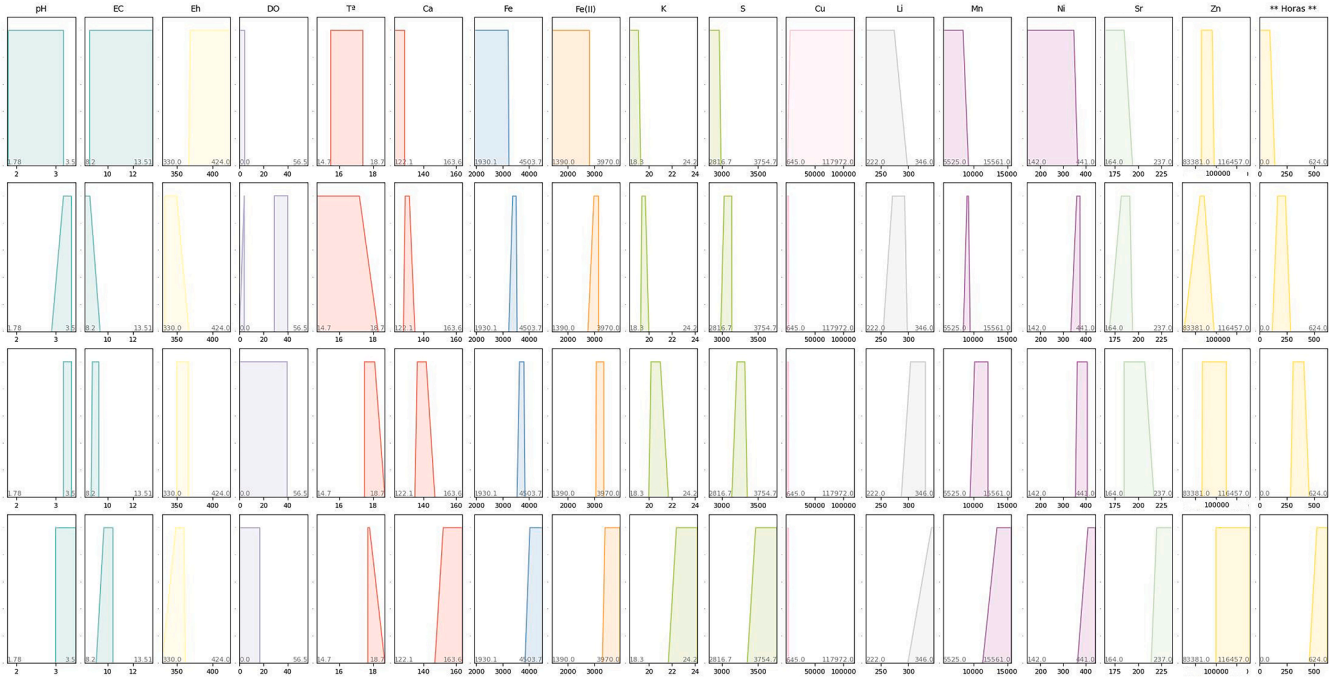

Fig. 2. Evolution of the parameters analyzed in the samples obtained in the PO solution (antecedents) in relation to the time the solution was in contact with the steel (consequents).

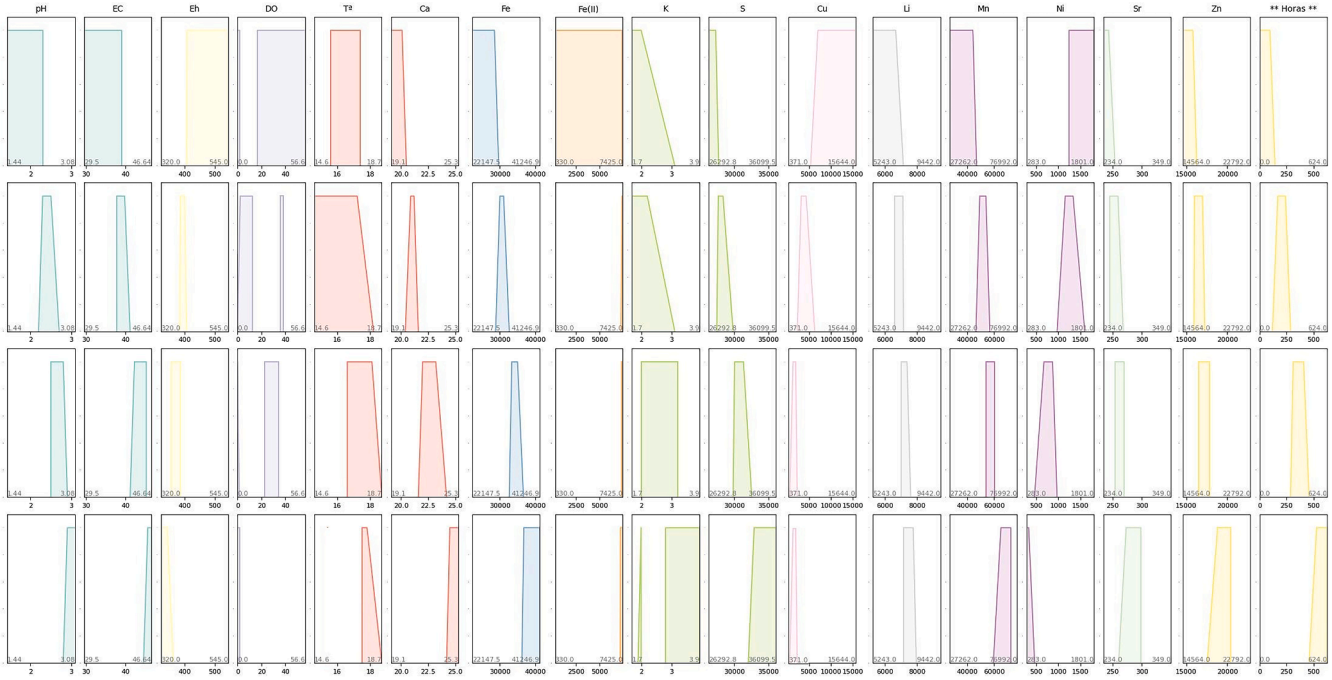

Fig. 3. Evolution of the parameters analyzed in the samples obtained in the pH solution (antecedents) in relation to the time the solution was in contact with the steel (consequents).

with a higher initial Fe^{3+}/Fe^{2+} ratio (PH). This behavior is attributed to the higher initial Fe^{3+} concentration in the latter, as well as the greater total acidity, which leads to an increase in hydroxylated species in solution. These species subsequently precipitate on the steel surface as oxyhydroxysulfates. On the other hand, the slight increase in Fe^{2+} in the distilled water solution, designed to replicate the effect of rainwater in the laboratory, indicates that oxidation of the steel plate has also occurred, albeit to a lesser extent than in the more acidic solutions.

In the solution with the highest Fe^{3+}/Fe^{2+} content (PH), the increase in Fe^{2+} is much more significant than in the solutions with a higher initial Fe^{2+}/Fe^{3+} ratio (PO and ST), which highlights the important role of steel corrosion and the action of acidophilic bacteria in this process. A noteworthy point is that the minimum dissolved oxygen (DO) value for all the acidic solutions is 0, as oxygen is consumed in the iron corrosion reactions. In the solution without acidophilic bacteria, the oxygen reduction rate is lower because these bacteria actively consume oxygen. Once the solution reaches anoxic conditions, the bacteria begin consuming Fe, which causes an increase in oxygen levels, followed by

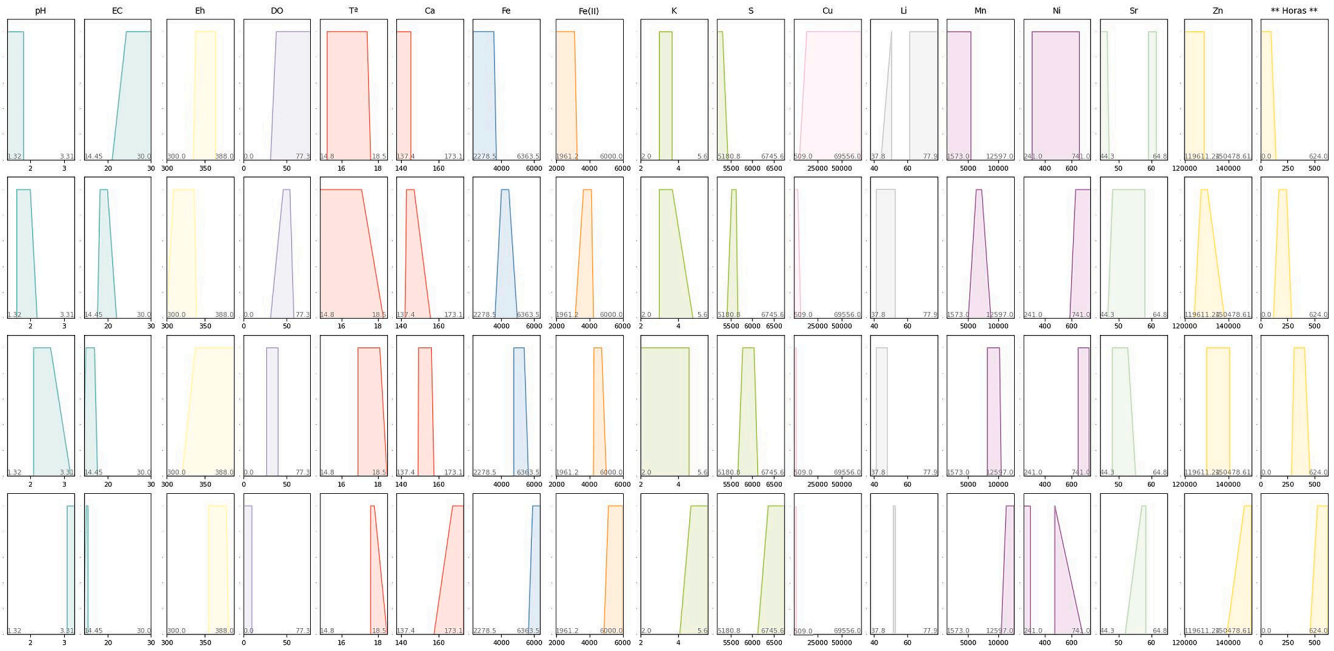

Fig. 4. Evolution of the parameters analyzed in the samples obtained in the ST solution (antecedents) in relation to the time the solution was in contact with the steel (consequents).

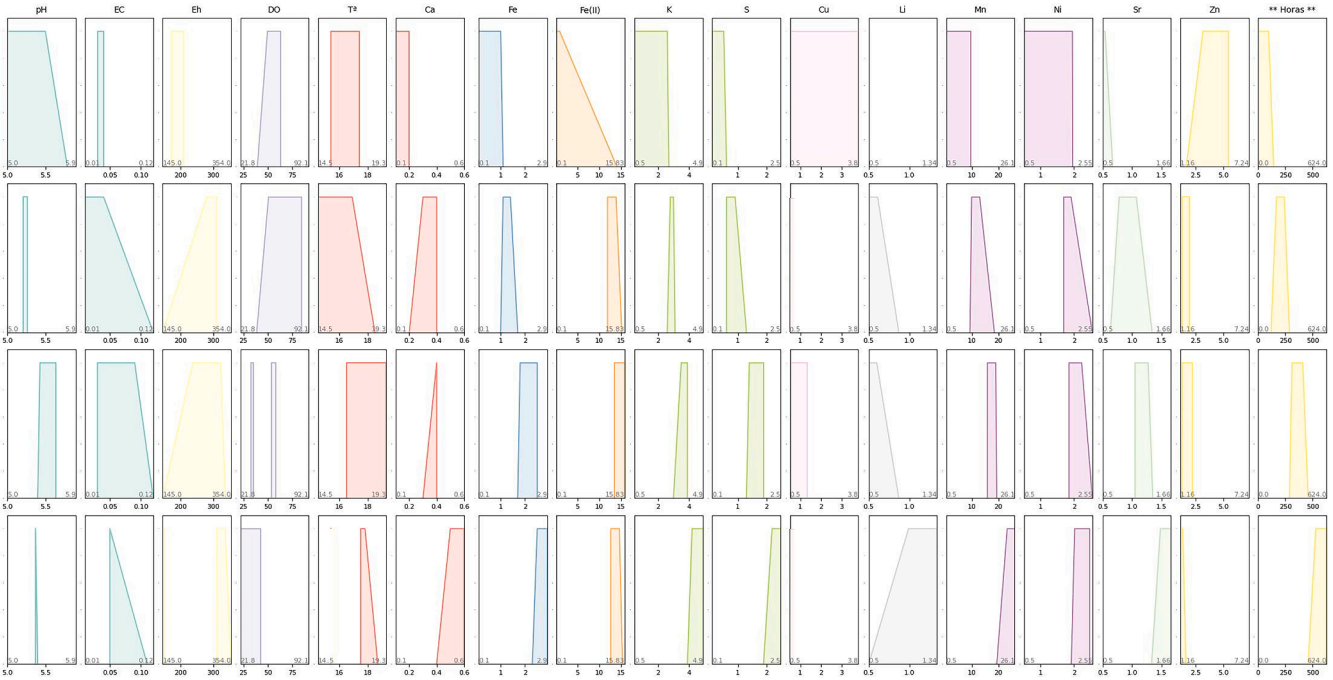

Fig. 5. Evolution of the parameters analyzed in the samples obtained in the distilled wáter solution (antecedents) in relation to the time the solution was in contact with the steel (consequents).

another decrease as the process continues.

Another significant observation is the sharp decrease in Cu concentration in all the solutions, which does not seem to depend on the presence of bacteria or the Fe^{2+}/Fe^{3+} ratio, but rather on the net acidity of the solution, which keeps Cu in solution for a longer time. Similarly, the variation in the concentration of S, present as sulfates, is comparable across the three acidic solutions, suggesting the absence of sulfate-reducing bacteria that would otherwise reduce SO_4^{2-} to HS^-.

Regarding the evolution of pH, in the solution without acidophilic bacteria (ST), a gradual increase is observed throughout the experiment, as the steel oxidation reactions, transitioning from Fe^{2+} to Fe^{3+} with proton consumption, occur more slowly. In contrast, in the solutions containing acidophilic bacteria (PO and PH), the pH increase is more abrupt during the initial hours of the experiment, indicating a faster rate of the involved reactions.

In this study, the effects of carbon steel corrosion in acid mine drainage have been evaluated using an innovative Artificial Intelligence (AI)-based approach, which has allowed for the comparison and validation of results obtained through classical statistics. This approach has provided deeper insights into the corrosion processes and the chemical-

biological interactions occurring in these solutions, highlighting the importance of initial composition and microbial activity in the evolution of the studied systems.

Funding: This work was supported by MCIU/AEI/10.13039/501,100,011,033/FEDER, UE, throughout the project PID2021–123130OB-I00. Also, this paper was partially funded by the projects: PID2020–119478GB-I00 and PID2022–137646OB-C31

CRediT authorship contribution statement

María Luisa de la Torre: Writing – original draft, Methodology, Investigation, Formal analysis, Conceptualization. **Javier Aroba:** Writing – review & editing, Software, Formal analysis. **Jose Miguel Davila:** Writing – review & editing, Investigation, Conceptualization. **Aguasanta M. Sarmiento:** Writing – review & editing, Project administration, Methodology, Investigation, Conceptualization.

Declaration of competing interest

The authors declare that they have no known competing financial interests or personal relationships that could have appeared to influence the work reported in this paper.

Data availability

Data will be made available on request.

References

[1] M. Banza, T. Seodigeng, S. Linda, M.M. Christian, S. Owona, P. Musampa, Batch and continuous fixed bed adsorption of copper (II) from acid mine drainage (AMD) using green and recyclable adsorbent from cellulose microcrystals (CMCs), J. Environ. Sci. Health, Part A 59 (9) (2024) 488–498, https://doi.org/10.1080/10934529.2024.2429284.

[2] M.B. Lindsay, M.C. Moncur, J.G. Bain, J.L. Jambor, C.J. Ptacek, D.W. Blowes, Geochemical and mineralogical aspects of sulfide mine tailings, Appl. Geochem. 57 (2015) 157–177, https://doi.org/10.1016/j.apgeochem.2015.01.009.

[3] A.M. Sarmiento, A.M. Rodriguez-Perez, J.M. Davila, Torre M.L. de la, Effect of acid mine drainage on the mechanical properties of AISI 1020 carbon steel and AW6060 aluminium, J. Mater. Res. Technol. 32 (2024) 541–549, https://doi.org/10.1016/j.jmrt.2024.07.099.

[4] R. Javaherdashti, H. Nikraz, On the role of deterioration of structures in their performance; with a focus on mining industry equipment and structures, Mater. Corros. 61 (2010) 885–890, https://doi.org/10.1002/maco.200905515.

[5] X. Li, D. Zhang, Z. Liu, Z. Li, C. Du, C. Dong, Materials science: share corrosion data, Nature 527 (2015) 441–442, https://doi.org/10.1038/527441a.

[6] J.E. Burwick, S. Sharma, C.M. Menge, A. Buldum, J.M. Senko, The influence of O2 availability and Fe(III) mineralogy on Fe metabolism by an acidophilic bacterial culture, Chemic. Geol. 547 (2017) 107–117, https://doi.org/10.1016/j.chemgeo.2017.03.023.

[7] V.K. Singh, A.L. Singh, R. Singh, A. Kumar, Iron oxidizing bacteria: insights on diversity, mechanism of iron oxidation and role in management of metal pollution, Environ. Sustain. 1 (2018) 221–231, https://doi.org/10.1007/s42398-018-0024-0.

[8] X. Liu, Y. Wang, Y. Song, W. Liu, J. Zhang, N. Li, K. Dong, Y. Cai, E. Han, The respective roles of sulfate-reducing bacteria (SRB) and iron-oxidizing bacteria (IOB) in the mixed microbial corrosion process of carbon steel pipelines, Corros. Sci. 240 (2024) 112479, https://doi.org/10.1016/j.corsci.2024.112479.

[9] M. Qiming, Q. Wenqing, Y. Binghua, L. Lin, Ferrous iron oxidation efficiency and kinetics by indigenous iron-oxidizing bacteria in acid mine drainage, Environ. Technol. Innov. 36 (2024) 103785, https://doi.org/10.1016/j.eti.2024.103785.

[10] D. Leduc, L.G. Leduc, G.D. Ferroni, Quantification of bacterial populations indigenous to acidic drainage stream, Water. Air. Soil. Pollut. 135 (2002) 1–21, https://doi.org/10.1128/aem.63.11.4516-4522.1997.

[11] N.O. San, H. Nazır, G. Dönmez, Microbially influenced corrosion and inhibition of nickel–zinc and nickel–copper coatings by Pseudomonas aeruginosa, Corros. Sci. 79 (2014) 177–183, https://doi.org/10.1016/j.corsci.2013.11.004.

[12] H. Liu, T. Gu, G. Zhang, W. Wang, S. Dong, Y. Cheng, H. Liu, Corrosion inhibition of carbon steel in CO2-containing oilfield produced water in the presence of iron-oxidizing bacteria and inhibitors, Corros. Sci. 105 (2016) 149–160, https://doi.org/10.1016/j.corsci.2016.01.012.

[13] A.M. Sarmiento, J.M. Nieto, M. Olias, C.R. Canovas, Hydrochemical characteristics and seasonal influence on the pollution by acid mine drainage in the Odiel river Basin (SW Spain), Appl. Geochem. 24 (4) (2009) 697–714, https://doi.org/10.1016/j.apgeochem.2008.12.025.

[14] A.M. Sarmiento, J.A. Grande, A.T. Luís, J.M. Dávila, J.C. Fortes, M. Santisteban, J. M. Curiel, M.L. de la Torre, E. Ferreira da Silva, Negative pH values in an open-air radical environment affected by acid mine drainage. Characterization and proposal of a hydrogeochemical model, Sci. Total Environ. 644 (2018) 1244–1253, https://doi.org/10.1016/j.scitotenv.2018.06.381.

[15] A. Barredo, N. Díaz-Rodríguez, J. Del Ser, A. Bennetot, S. Tabik, A. Barbado, S. Garcia, S. Gil-Lopez, D. Molina, R. Benjamins, R. Chatila, F. Herrera, Explainable Artificial Intelligence (XAI): concepts, taxonomies, opportunities and challenges toward responsible AI, Info. Fus. 58 (2020) 82–115, https://doi.org/10.1016/j.inffus.2019.12.012.

[16] T.C. Tang, L.C. Chi, Predicting multilateral trade credit risks: comparisons of Logit and Fuzzy logic-based models using ROC curve analysis, Expert. Syst. Appl. 28 (3) (2005) 547–556, https://doi.org/10.1016/j.eswa.2004.12.016.

[17] Y. Yi, J. Sun, S. Zhang, Z. Yang, Assessment of Chinese sturgeon habitat suitability in the Yangtze River (CHINA): comparison of generalized additive model, data-driven fuzzy logic-based model, and preference curve model, J. Hydrol. 536 (2016) 447–456, https://doi.org/10.1016/j.jhydrol.2016.03.005.

[18] R. Fernández, I. Brito, J. Aroba, F. Gómez, S. Rodríguez, J. de la Rosa, Assessment of ultrafine particles and noise measurements using fuzzy logic and data mining techniques, J. Sci. Total Environ. (512-513) (2015) 103–113, https://doi.org/10.1016/j.scitotenv.2015.01.036.

[19] A. Fernández, F. Herrera, O. Cordón, M.J. del Jesus, F. Marcelloni, Evolutionary fuzzy systems for explainable artificial intelligence: why, when, what for, and where to? IEEe Comput. Intell. Mag. 14 (1) (2019) 69–81, https://doi.org/10.1109/MCI.2018.2881645.

[20] AM. Julfikhsan, G. Nenad, K. Seong-Hoon, AI-assisted ultrasonic wave analysis for automated classification of steel corrosion-induced concrete damage, Autom. Constr. 167 (2024) 105704, https://doi.org/10.1016/j.autcon.2024.105704.

[21] B. Martín del Brío, A. Sanz-Molina, Redes Neuronales y Sistemas Borrosos, Madrid, Ra-Ma, 2006.

[22] Torre M.L. de la, J.A. Grande, T. Valente, E. Perez-Ostalé, M. Santisteban, J. Aroba, I. Ramos, Definition of redox and pH influence in the AMD mine system using a fuzzy qualitative tool (Iberian Pyrite Belt, SW Spain), Environ. Sci. Poll. Res. 23 (2016) 5451–5458, https://doi.org/10.1007/s11356-015-5718-6.

[23] A.T. Luís, J.A. Grande, J.M. Davila, J. Aroba, N. Durães, S.F.P. Almeida, M.L. de la Torre, A.M. Sarmiento, J.C. Fortes, E. Ferreira da Silva, M. Santisteban, Application of fuzzy logic tools for the biogeochemical characterisation of (un)contaminated waters from Aljustrel mining area (South Portugal), Chemosphere 211 (2018) 736–744, https://doi.org/10.1016/j.chemosphere.2018.07.194.

[24] C. Jui-Sheng, N. Ngoc-Tri, K.C. Wai, The use of artificial intelligence combiners for modeling steel pitting risk and corrosion rate, Eng. Appl. Artif. Intell. 65 (2017) 471–483, https://doi.org/10.1016/j.engappai.2016.09.008.

[25] L. Qiang, W. Dongxu, Z. Mingyu, Y. Minghao, T. Jianfeng, Z. Kai, Modeling the corrosion rate of carbon steel in carbonated mixtures of MDEA-based solutions using artificial neural network, Process Safet. Environ. Prot. 147 (2021) 300–310, https://doi.org/10.1016/j.psep.2020.08.035.

[26] H.K. Ali, L. Bing, N.A. Ahmed, H. Zhongzhi, X. Ying, T. Junlei, Enhanced prediction of corrosion rates of pipeline steels using simulated annealing-optimized ANFIS models, Results. Eng. 24 (2024) 102853, https://doi.org/10.1016/j.rineng.2024.102853.

[27] O. Bamshad, B. Jamhiri, A. Habibi, S. Salehi, M. Aziminezhad, M. Mahdikhani, Predicting corrosion of recycled aggregate concrete under sulfuric acid rain using machine learning and uncertainty analysis, Constr. Build. Mater. 438 (2024) 137146, https://doi.org/10.1016/j.conbuildmat.2024.137146.

[28] A. Mohammadreza, M. Ramin, C. Martin, B. Bruce, S. Marc, N. Srdjan, M.V. Silvia, S. Sumit, Machine learning modeling of time-dependent corrosion rates of carbon steel in presence of corrosión inhibitors, Corros. Sci. 193 (2021) 109904, https://doi.org/10.1016/j.corsci.2021.109904.

[29] N. Rosette, J. Wei, M. Elyse, M. Jean, N. Ferdinand, N. Ritha, Intelligent damage diagnosis in bridges using vibration-based monitoring approaches and machine learning: a systematic review, Results. Eng. 16 (2022) 100761, https://doi.org/10.1016/j.rineng.2022.100761.

[30] H. Soroosh, P. Shamim, B. Abdel-Hakim, A.H. Lucas, Application of machine learning for the classification of corrosion behavior in different environments for material selection of stainless steels, Comput. Mater. Sci. 228 (2023) 112352, https://doi.org/10.1016/j.commatsci.2023.112352.

[31] I.M. Salim, H.A. Faiz, A. Suleiman, S.I Haruna, I.l.A. Shaban, S.I. Abba, Implementation of hybrid neuro-fuzzy and selfturning predictive model for the prediction of concrete carbonation depth: A soft computing technique, Results. Eng. 10 (2021) 100228, https://doi.org/10.1016/j.rineng.2021.100228.

[32] S. Uzair, A. Aqeel, H. Imtiyaz, S. Muhammad, M.A. Hafiz, Y. Wei-Mon, Explainable artificial intelligence-based insights into the corrosion behavior of WS2/AZ91 composites subjected to severe deformation conditions, Results. Eng. 21 (2024) 101897, https://doi.org/10.1016/j.rineng.2024.101897.

[33] W. Wang, J. Cao, M. Zeng, Y. Qiao, A comprehensive literature mining and machine learning to decipher and predict effects of concrete materials on concrete corrosion of sewer pipe, Urban. Water. J. (2024) 1–18, https://doi.org/10.1080/1573062X.2024.2352599.

[34] J. Aroba, Advances in the Decision Making in Software Development Projects, University of Sevilla, Spain, 2003. PhD Thesis.

[35] S. Orandi, D.M. Lewis, Synthesising acid mine drainage to maintain and exploit indigenous mining micro-algae and microbial assemblies for biotreatment investigations, Environ. Sci. Pollut. Res. 20 (2012) 950–956, https://doi.org/10.1007/s11356-012-1006-x.

[36] J. Rodier, B. Legube, N. Merlet, L'analyse De L'eau, Dunod, Paris, 2016.

[37] D.L. Parkhurst, User's guide to PHREEQC–a computer program for speciation, reactionpath, 1D-transport, and inverse geochemical calculations, Water-Resourc. Investig. Report 99 (1999) 4259, https://doi.org/10.3133/wri954227.

[38] J.W Ball, D.K. Nordstrom, User's manual for WATEQ4F, with revised thermodynamic data base and text cases for calculating speciation of major, trace, and redox elements in natural Waters, USGS Numb. Ser.. Open-File Report (1991) 91–183, https://doi.org/10.3133/ofr91183.
[39] C.S. Kirby, III C.A. Cravotta, Net alkalinity and net acidity 2: practical considerations, Appl. Geochem. 20 (2005) 1941–1964, https://doi.org/10.1016/j.apgeochem.2005.07.003.
[40] M. Farkhadov, A. Eliseev, N. Petukhova, Explained artificial intelligence helps to integrate artificial and Human intelligence into medical diagnostic systems: analytical review of publications, in: IEEE 14th International Conference on Application of Information and Communication Technologies (AICT), Tashkent, 2020, pp. 1–4, https://doi.org/10.1109/AICT50176.2020.9368576.
[41] R. González-Alday, E. García-Cuesta, C.A. Kulikowski, V. Maojo, A scoping review on the progress, applicability, and future of explainable artificial intelligence in medicine, Appl. Sci. 13 (19) (2023) 10778, https://doi.org/10.3390/app131910778.
[42] L. Kaufman, P.J. Rousseeuw, Finding Groups in Data: An Introduction to Cluster Analysis, Wiley & Sons, New York, NY, USA, 2009. ISBN 0-471-73578-7.
[43] R. Hathaway, J. Bezdek, Switching regression models and fuzzy clustering, IEEE Trans. Fuzzy Syst. 1 (1993) 195–204, https://doi.org/10.1109/91.236552.
[44] M. Sugeno, A. Yasukawa, A fuzzy-logic based approach to qualitative modeling, IEEE Trans. Fuzzy Syst. 1 (1993) 7e31.
[45] J.C. Bezdek, Pattern Recognition with Fuzzy Objective Function Algorithm, Plenum Press, New York, 1981.
[46] F. Höppner, F. Klawonn, A contribution to convergence theory of fuzzy c-means and derivatives, IEEE Trans. Fuzzy Syst. 11 (2003) 682–694, https://doi.org/10.1109/tfuzz.2003.817858.
[47] Y. Fukuyama, M. Sugeno, A new method of choosing the number of clusters for fuzzy means method, in: Proceedings of the 5th Fuzzy Systems Symposium, 1989, pp. 247–250.
[48] U. Lueder, G. Druschel, D. Emerson, A. Kappler, C. Schmidt, Quantitative analysis of O2 and Fe2+ profiles in gradient tubes for cultivation of microaerophilic iron (II)-oxidizing bacteria, FEMS. Microbiol. Ecol. 94 (2) (2018) fix177, https://doi.org/10.1093/femsec/fix177.
[49] J. Sánchez-España, A. Ilin, I. Yusta, Metallic copper (Cu[0]) obtained from Cu2+-rich acidic mine waters by two different reduction methods: crystallographic and geochemical aspects, Minerals 12 (2022) 322, https://doi.org/10.3390/min12030322.
[50] C.L. Caldeira, V.S.T. Ciminelli, K. Osseo-Asare, The role of carbonate ions in pyrite oxidation in aqueous systems, Geochim. Cosmochim. Acta 74 (2010) 1777–1789, https://doi.org/10.1016/j.gca.2009.12.014.